

# Finite Element Wear Behavior Modeling of Al/Al<sub>2</sub>SiO<sub>5</sub>/C Chilled Hybrid Metal Matrix Composites (CHMMCs)

Joel Hemanth

Rajiv Gandhi Institute of Technology, Bangalore, Karnataka, India.  
E-mail: joelhemanth@hotmail.com  
Received July 8<sup>th</sup>, 2010; revised August 12<sup>th</sup>, 2010; accepted May 21<sup>st</sup>, 2011.

## ABSTRACT

*This paper describes research on aluminum based metal matrix hybrid composites reinforced with kaolinite (Al<sub>2</sub>SiO<sub>5</sub>) and carbon (C) particulates cast using high rate heat transfer technique during solidification by employing metallic, non-metallic and cryogenic end chills. The effect of reinforcement and chilling on strength, hardness and wear behavior are discussed in this paper. It is discovered that cryogenic chilled MMCs with Al<sub>2</sub>SiO<sub>5</sub>-9 vol.%/C-3 vol.% dispersoid content proved to be the best in enhancing the mechanical and wear properties. A physically based Finite element (FE) model for the abrasive wear of the hybrid composite developed is based on the mechanisms associated with sliding wear of ductile aluminum matrix of the composite containing hard Al<sub>2</sub>SiO<sub>5</sub> and soft carbon (dry lubricant) reinforcement particles. Finally the results reveal that there is a good agreement that exists between the simulated (FE) values and those of the experimental values, proving the suitability of the boundary conditions.*

**Keywords:** Aluminum, Composites, Casting, Hybrid and Wear

## 1. Introduction

Reinforced hybrid metal matrix composites (HMMC), constituted of high-strength metallic alloys reinforced with two dispersoids are advanced materials that have emerged from the perpetual need of lighter-weight, higher-performance components more recently used in automotive applications. Indeed, these new materials offer promising perspectives in assisting automotive engineers to achieve improvement in vehicle fuel efficiency. Their destructive properties of high stiffness, high strength and low density have prompted an increasing number of applications for these materials. Several of these applications require enhanced friction and wear performances.

Wear of components is often a critical factor influencing the product service life and most confident knowledge about the friction pair tribological behavior can be achieved by making wear experiments. Wear takes place when surfaces of mechanical components contact each other hence its prediction is therefore an important part of engineering. In order to predict wear and eventually the life-span of complex mechanical systems, several hundred thousand operating cycles have to be simulated.

Hence, wear and the calculation of wear between surfaces in contact has not been a concern in the finite element realm. Therefore finite element (FE) post-processor is the optimum choice, considering the computational expense. Therefore a FE software MSC-Marc has been used in this research to initiate a discussion of a procedure for calculation of wear.

Hence the objective of this research is twofold, first to develop chilled hybrid MMC using kaolinite (Al<sub>2</sub>SiO<sub>5</sub>, a hard ceramic) and carbon (dry lubricant) as reinforcements, second to analyze the wear performance of the hybrid MMC developed experimentally as well as by FE modeling.

## 2. Literature Review

In recent years there has been a great deal of interest in developing metal matrix composites (MMC) because of their unique mechanical properties such as light weight and high elastic modulus. The common fabrication routes of particulate reinforced MMCs include spray deposition, liquid metallurgy and powder metallurgy [1,2]. Since expensive equipment is required and the processing routes are usually complex, the cost to produce MMCs by these methods is high, which has limited the applica-

tions of MMC materials. Presently, the bonding technique of hot and cold rolling process developed to fabricate particular reinforced MMCs involves complexities [3-7]. Several other processes used to produce discontinuous MMCs also include rheocasting, compocasting and squeeze casting [8-11]. Many reports on the characterization of mechanical properties of discontinuous MMCs have been available [12-15]. According to them, mechanical properties such as Young's modulus and strength, have been improved about 20% - 40% by incorporation of reinforcements. However, ductility has deteriorated remarkably with increasing content of reinforcements [16-18]. There are many micro structural variables, such as the ageing condition of the matrix alloy, the material used as reinforcement, the volume fraction and the size of the particulates, and each of these may effect the mechanical properties of the composite [19-21]. Reinforcing an Al alloy with particulates yields a composite that displays the superior physical and mechanical properties of both the metal matrix and the dispersoid. On a weight-adjusted basis, many Al-based metal matrix composites (MMCs) can outperform cast steel, Al, Mg and virtually any other reinforced metal or alloy in a wide variety of applications. Hence, it seems probable that such MMCs will replace conventional materials in many commercial and industrial applications in the near future [22-25].

Wear is an important in any structure subjected to repeated loadings and may be critical for certain tribological applications. In this research, a proper procedure is proposed whereby the effects of wear may be calculated and included in the overall analysis of the structure. The famous Archard equation is used as the basis for calculating wear strain which is used to modify the elastic strain of an element in an explicit manner [26].

A wear simulation approach based on Archard's wear law is implemented in an FE post processor that works in association with commercial FE package MSC-Marc for solving the general deformable contact problems. Here local wear is computed and then integrated over the sliding distance using the Euler integration scheme. The wear simulation tool works with FE simulation with surface geometries to get realistic contact pressure distribution on the contacting surfaces. The wear on both the interacting surfaces are computed using the contact pressure distribution [27-29].

It is well known that Al alloys that freeze over a wide range of temperature are difficult to feed during solidification. The dispersed porosity caused by the pasty mode of solidification can be effectively reduced by the use of chills. Chills extract heat at a faster rate and promote directional solidification. Therefore chills are widely used by foundry engineers for the production of sound

and quality castings. There have been several investigations [30-32] on the influence of chills on the solidification and soundness of alloys. With the increase in the demand for quality composites, it has become essential to produce Al composites free from unsoundness.

Search of open literature indicates that, so far number of Al based MMCs including chilled MMCs are being developed but no work has been done in this field. Hence the present research is undertaken to fill the void and to investigate the integrated properties of chilled Al-alloy/Al<sub>2</sub>SiO<sub>5</sub>/C HMMCs. Among all the reinforcements used in Al based composites only combination of particulates and chilling in the present investigation has shown their potential superiority in improving mechanical properties, microstructure with noticeable weight savings.

#### Relevance of the Research

In this research both experimental and Finite Element (FE) modeling is developed that are used to identify the abrasive wear of the composite developed. This FE software (MSC Marc) is well suited for solving of contact problems as well as the wear simulation. Here, a pin on disc un-lubricated contact was analyzed experimentally with FE modeling. This model is based on the assumption that any portion of the reinforcement that is removed as wear debris cannot contribute to the wear resistance of the composite material developed. Critical variables describing the role of the reinforcement such as relative size, hardness and nature of the matrix material/reinforcement interface are characterized. Predictions are compared with the results of experimental two body (pin on disc) abrasive wear tests performed on a model developed.

### 3. Experimental Procedure

#### 3.1. Fabrication of Al/Al<sub>2</sub>SiO<sub>5</sub>/C Hybrid Chilled MMCs

The chemical composition of the aluminum alloy (LM 13) used as the matrix material is given in **Table 1**.

In this investigation, the amount of Al<sub>2</sub>SiO<sub>5</sub>/C particulates dispersed in the matrix are Al<sub>2</sub>SiO<sub>5</sub>-3/C-3 vol.%, Al<sub>2</sub>SiO<sub>5</sub>-6/C-3 vol.%, Al<sub>2</sub>SiO<sub>5</sub>-9/C-3 vol.% and Al<sub>2</sub>SiO<sub>5</sub>-12/C-3 vol.% (combination of dispersoid varies from 3 to 12 vol% in steps of 3% of Al<sub>2</sub>SiO<sub>5</sub>) respectively. The size of Al<sub>2</sub>SiO<sub>5</sub>/C particulates dispersed is between 30 and 80 μm. After melting the matrix material in a furnace at around 720°C in an inert atmosphere, Al<sub>2</sub>SiO<sub>5</sub> and C particulates preheated to 600°C were introduced evenly into the molten metal alloy by means of special feeding (sandwich technique) attachments. The melt was next poured into a sand mould containing different chills (each 25 mm thick) attached to it at one end. Sub zero copper end chill of thickness 25 mm was used in which

**Table 1. Chemical composition of matrix material (Al-alloy LM 13).**

Elements	Zn	Mg	Si	Ni	Fe	Mn	Al
% by wt	0.5	1.4	12	1.5	1.0	0.5	Bal

arrangements were made to circulate liquid nitrogen (at  $-90^{\circ}\text{C}$ ) to study the effect of heat capacity on mechanical and micro structural behavior. The chills used were 170 mm long, 35 mm high and 25 mm thick. The moulds were produced according to AFS standards of dimension  $225 \times 150 \times 25$  mm. Specimens for all the tests were selected only at the chill end of the casting and all the specimens were heat-treated by aging before testing.

- Chills used: 1. Sub zero copper chill  
2. Metallic chill (copper)  
3. Non metallic chill (graphite)

### 3.2. Properties of Dispersoid: Al<sub>2</sub>SiO<sub>5</sub> (Kaolinite)

Density: 3.9 gm/cc, Hardness: 430 BHN, Chemical formula: Al<sub>2</sub>SiO<sub>5</sub>

Melting point: 2050°C, Space group: P1 Triclinic, Young's modulus: 89 GPa,

Chemical composition: SiO<sub>2</sub>, Al<sub>2</sub>O<sub>3</sub>, Fe<sub>2</sub>O<sub>3</sub>, TiO<sub>2</sub>, MgO.

### 3.3. Testing Procedure

Microscopic examination was conducted on all the specimens using scanning electron microscope (SEM) as well as using Neophot-21 metallurgical microscope. Dry wear tests were conducted at room temperature as per ASTM D5963-97 standards using the computerized pin on disc wear tester manufactured by Riken-Ogoshi & Co., Korea. The studied configuration is a pin of 6 mm diameter on plane contact, where as the plane is the AISI 5210 steel. Wear tests using volume loss method were performed at different loads (10 to 50 N in steps of 10 N) for a time period of 300 seconds. Hardness and strength tests (on AFS standard tensometer specimen) were performed using Vickers hardness tester and Instron testing machine.

### 3.4. Pin on Disc FE Model for Wear Testing

The model presented in this research (refer **Figure 1**) consists of two bodies, the lower one is a rotating disc (AISI 52100) steel and top of it is a rigid body (pin of 6 mm diameter) contact surface. The rigid contact surface is used to apply the load to the rotating surface. Here the famous Archard [33] approach taking into account the wear process is introduced to formalize the wear kinetics. This model is developed based on equal and steady state wear rate assumption with simplified geometry in which abrasive medium particle acting on composite containing reinforcements.

Here the analysis is performed in three load steps: 1)

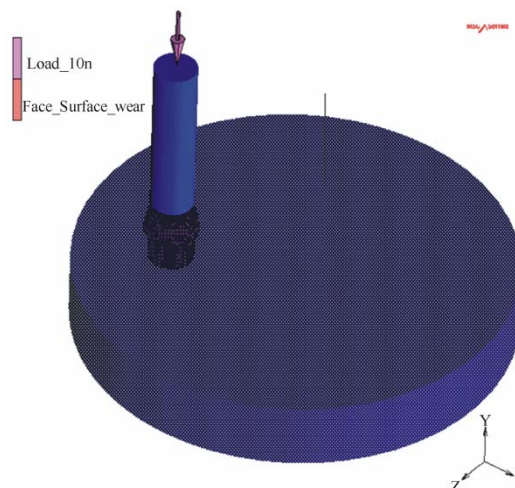


**Figure 1. Pin on disc model for measuring wear rate.**

Displacement of the pin to generate the contact 2) The load step which converts displacement to load after contact has been established and 3) The static loading step in which a group of load steps each with an incremental time that represents the repetition of the load to calculate the wear over a time period.

In this investigation, predictions are compared with the results of experimental two-body (pin on disc) abrasive wear tests performed on the same chilled Al<sub>2</sub>SiO<sub>5</sub>/C MMC specimen.

## 4. Results and Discussion.

In the present investigation, of all the chills, sub zero copper end chill was found to be the most effective because of its high VHC. Dispersoid content up to Al<sub>2</sub>SiO<sub>5</sub>-9/C-3 vol.% was found to increase the mechanical properties (strength and hardness) and therefore it is considered to be the optimum limit. Hence the present discussion is mainly focused on sub zero copper chilled MMC with Al<sub>2</sub>SiO<sub>5</sub>-9 /C-3 vol.% dispersoid content

### 4.1. Micro Structural Studies

**Figures 2(a-c)** show the microstructure of chilled hybrid MMCs containing Al<sub>2</sub>SiO<sub>5</sub>-9/C-3 vol.% dispersoid, cast using different chills. Micro structural examination of chilled MMCs is discussed in terms of distribution of reinforcement and reinforcement matrix interfacial bonding. It is observed from these figures that for all the chilled MMCs there is a uniform distribution of dispersoid and good bonding with the matrix. Micro structural studies conducted on the composite containing Al<sub>2</sub>SiO<sub>5</sub>-9/

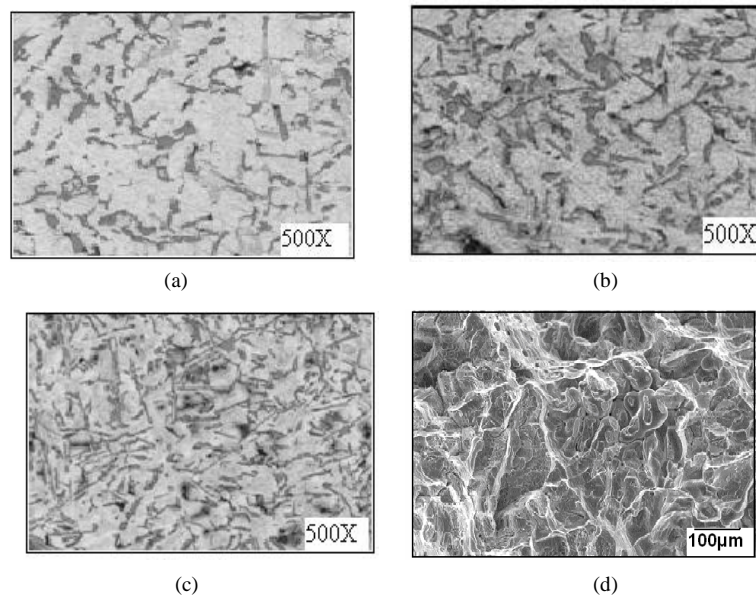


**Figure 2. Microstructure of chilled hybrid MMCs containing Al<sub>2</sub>SiO<sub>5</sub>/C-3 vol.% dispersoid, cast using different chills. (a) Graphite chilled MMC; (b) Copper chilled MMC; (c) Sub zero chilled MMC; (d) SEM fractograph of hybrid MMC containing Al<sub>2</sub>SiO<sub>5</sub>-9/C-3 vol.% dispersoid, cast using sub zero chill.**

C-3 vol.% dispersoid content cast using sub zero chill revealed limited extent of clusters, good reinforcement-matrix interfacial integrity, and significant grain refinement with minimal porosity (**Figure 2(c)**). This is due to gravity of Al<sub>2</sub>SiO<sub>5</sub> particulates associated with judicious selection of stirring parameters (vortex route), good wetting of pre heated reinforcement by the matrix melt. **Figures 2(a,b)** show graphite and copper chilled MMCs in which there is an increase in the size of the grains and of course with uniform distribution of the dispersoid. Grain refinement in all these chilled hybrid composites can primarily be attributed to capability of Al<sub>2</sub>SiO<sub>5</sub> and carbon particulates to nucleate aluminum grains during directional solidification and restricted growth of recrystallized aluminum grains because of presence of finer reinforcement and chilling. Interfacial integrity between matrix and the reinforcement was assessed using scanning electron microscope of the fractured surface (**Figure 2(d)**) to analyze the interfacial de-bonding at the particulate-matrix interface. Here also the result revealed that a strong bond exists between the interfaces as expected from metal/oxide systems [34].

Micro and macro tests conducted on chilled MMCs reveal that, high rate heat transfer during solidification (*i.e.*, effect of chilling) of the composite in this investigation leads to stronger bond between dispersoid and the matrix. This may be one of the main reasons for increase of strength, hardness and wear resistance of the composite developed. The result of micro structural studies of

chilled MMCs however did not reveal presence of any micro-pores or shrinkage cavity.

#### 4.2. Heat Treatment and Hardness

All the test samples before mechanical testing were subject to aging process. Therefore, if all other factors are kept constant, the aging rate of a composite is generally faster than that of the matrix alloy [35]. After solution treatment, optimum aging conditions can be determined by observing the hardness of the MMCs cast using chills for different aging durations. It is known that the optimum aging conditions are strongly dependent upon the amount of dispersoid present [36]. It can be seen that for each MMC, as the aging time increases, the hardness of the MMCs increases to a peak value and then drops again. As Al<sub>2</sub>SiO<sub>5</sub>/C content is increased, there is a tendency for the peak aging time to be reduced because dispersoids provide more nucleation sites for precipitation. As expected, for any fixed aging temperature and duration, increasing the Al<sub>2</sub>SiO<sub>5</sub>/C content causes the hardness of the MMC to increase since Al<sub>2</sub>SiO<sub>5</sub>/C combination of particulates are so much harder than the aluminum alloy matrix.

**Figure 3** shows hardness of chilled hybrid MMCs cast using various types of chills. The results of micro hardness test (HV) conducted on chilled MMCs samples revealed an increasing trend in matrix hardness with an increase in reinforcement content (up to 9 vol%). Results of hardness measurements also revealed that the type of chill has an effect on hardness of the composite. This

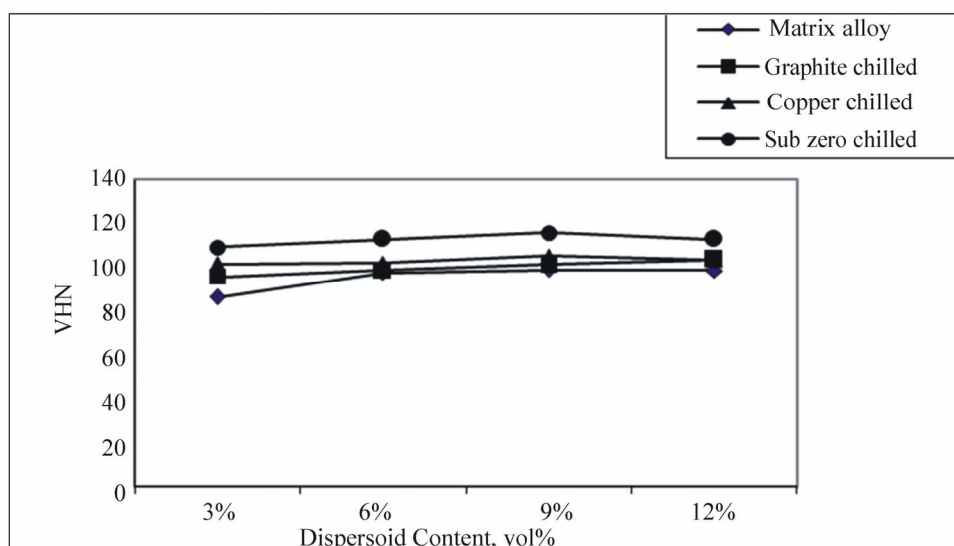


Figure 3. Hardness Vs dispersoid content of chilled hybrid MMCs.

significant increase in the hardness can be attributed primarily to presence of harder Al<sub>2</sub>SiO<sub>5</sub> ceramic particulates in the matrix, a higher constraint to the localized deformation during indentation due to their presence and reduced grain size due to chilling. In ceramic-reinforced composite, there is generally a big difference between the mechanical properties of the dispersoid and those of the matrix. These results in incoherence and a high density of dislocations near the interface between the dispersoid and the matrix [37]. Precipitation reactions are accelerated because of incoherence and the high density of dislocations act as heterogeneous nucleation sites for precipitation [38].

#### 4.3. Ultimate Tensile Strength (UTS) of the Composite

Figure 4 shows the effect of dispersoid content on UTS for various MMCs cast using different types of chills of thickness 25 mm. It is observed that UTS is again maximum for the hybrid composite containing Al<sub>2</sub>SiO<sub>5</sub>-9/C-3 vol.% cast using sub zero chill. Further, it may be observed from Figure 4 that, the effect of increasing the VHC of the chill increases UTS. In most cases, ceramic reinforced MMCs have superior mechanical properties to the un-reinforced matrix alloy because these MMCs have high dislocation densities due to dislocation generation as a result of differences in coefficient of thermal expansion [39]. As in the study however, with the incorporation of carbon particulates aimed at improving wear property has little effect on mechanical properties *i.e.*, UTS and hardness is due to addition of combination of dispersoids. However, in a hybrid composite, UTS and hardness of Al/Al<sub>2</sub>SiO<sub>5</sub>/C are slightly increased by increasing the

addition of Al<sub>2</sub>SiO<sub>5</sub> particulates. This shows that, carbon additions were seen to be less effective in strengthening than Al<sub>2</sub>SiO<sub>5</sub> particulates alone. It can be considered that carbon particulates in the hybrid system wet with the molten aluminum alloy and also react with the matrix alloy to form hard and brittle aluminum carbide (Al<sub>4</sub>C<sub>3</sub>) at high temperatures. From the results, the mechanical characterization of chilled Al/Al<sub>2</sub>SiO<sub>5</sub>/C hybrid MMCs can be summarized as follows: Carbon particulates have little effect on tensile properties but has more effect on wear behavior, where as Al<sub>2</sub>SiO<sub>5</sub>/C contributes for strength, hardness as well as for wear.

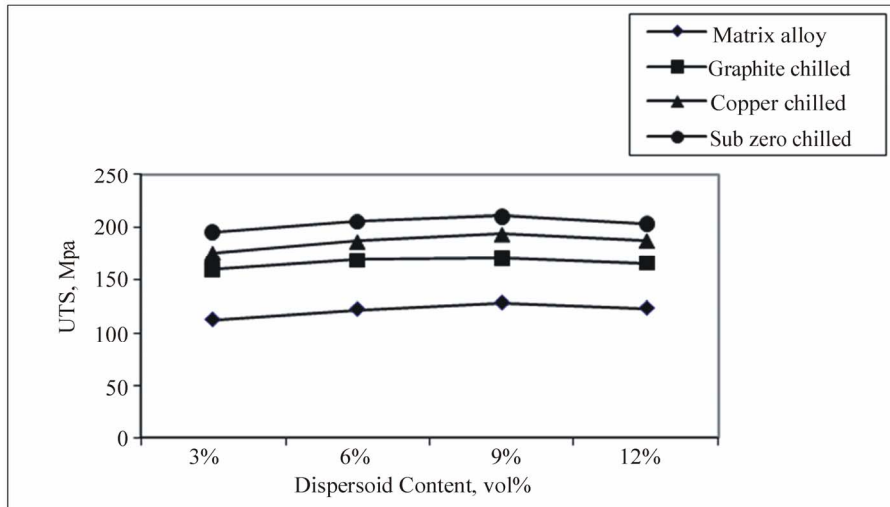
#### 4.4. Experimental Analysis of Wear Behavior

Figure 5 shows the effect of load on the wear rate of matrix alloy and different chilled hybrid Al/Al<sub>2</sub>SiO<sub>5</sub>/C MMCs. It can be seen from these figures that as the load and dispersoid content increases, the wear rate of the composite improves remarkably. It is observed from Figure 5(a) that the matrix alloy exhibits the highest wear due to its low hardness followed by graphite, copper and sub zero chilled MMCs in that order. It is also noticed from these figures that, increasing the dispersoid content up to Al<sub>2</sub>SiO<sub>5</sub>-9 vol.%/C-3 vol.% (addition beyond this limit deteriorate the properties) leads to a sharp reduction in wear rate. Therefore, the increased wear resistance of the composite, reinforced with Al<sub>2</sub>SiO<sub>5</sub>/C is attributing to the increase of hardness and UTS of the matrix phase and the low wear of Al<sub>2</sub>SiO<sub>5</sub> particles. The abrasive wear mechanism described by Rabinowicz [40] and sliding wear due to adhesion given by Archard [41] both indicate that the wear rate depends on the hardness of the material *i.e.*, volumetric loss of the material is inversely propor-

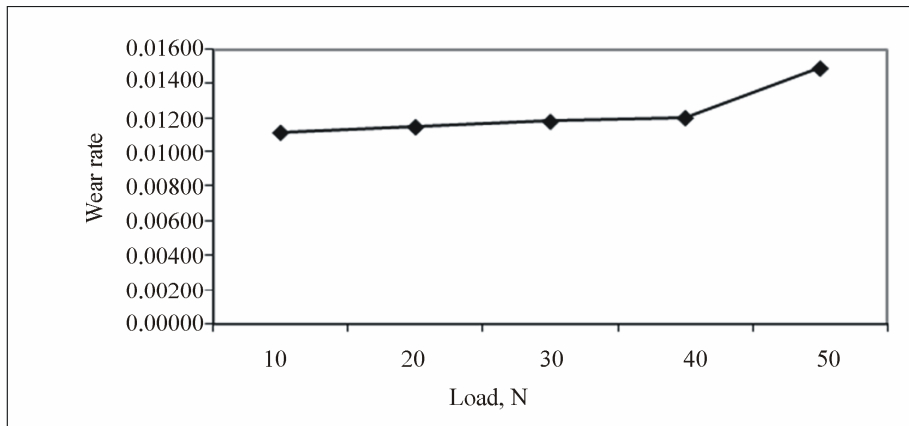
tional to the hardness value of the material. The experimental data of this research work as shown in **Figures 5(a-d)** and **Figure 3** (hardness plot) correlate well with

Rabi-nowicz wear mechanism.

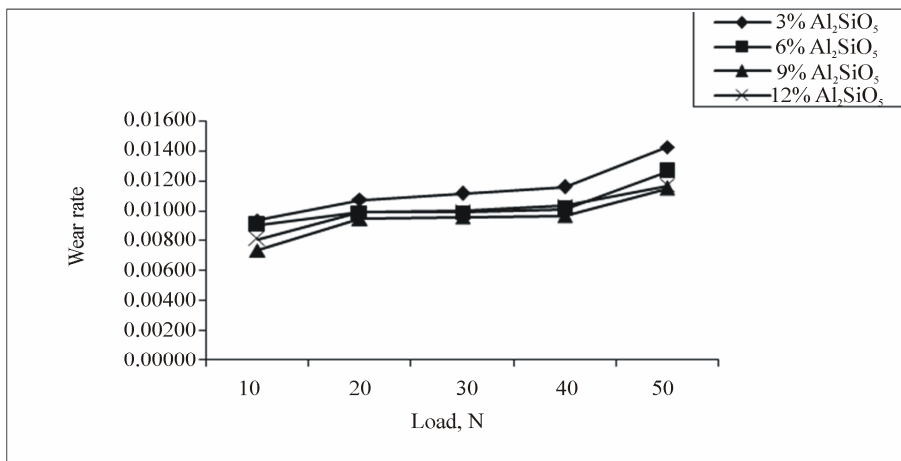
Also from **Figure 5(d)** it is seen that the wear rate for sub zero chilled MMC containing Al<sub>2</sub>SiO<sub>5</sub>-9/C-3 vol.%



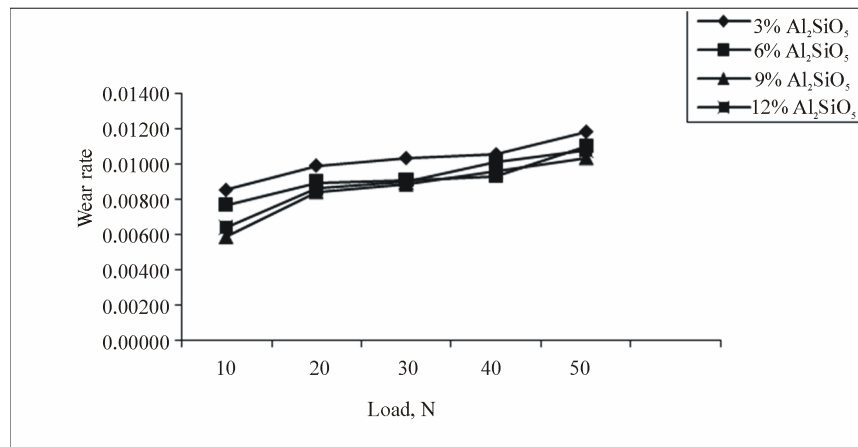
**Figure 4. Strength Vs dispersoid content of chilled hybrid MMCs.**



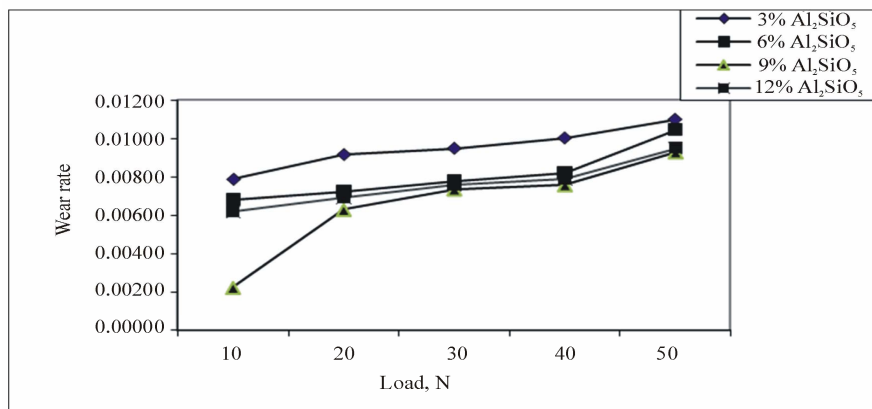
(a)



(b)



(c)



(d)

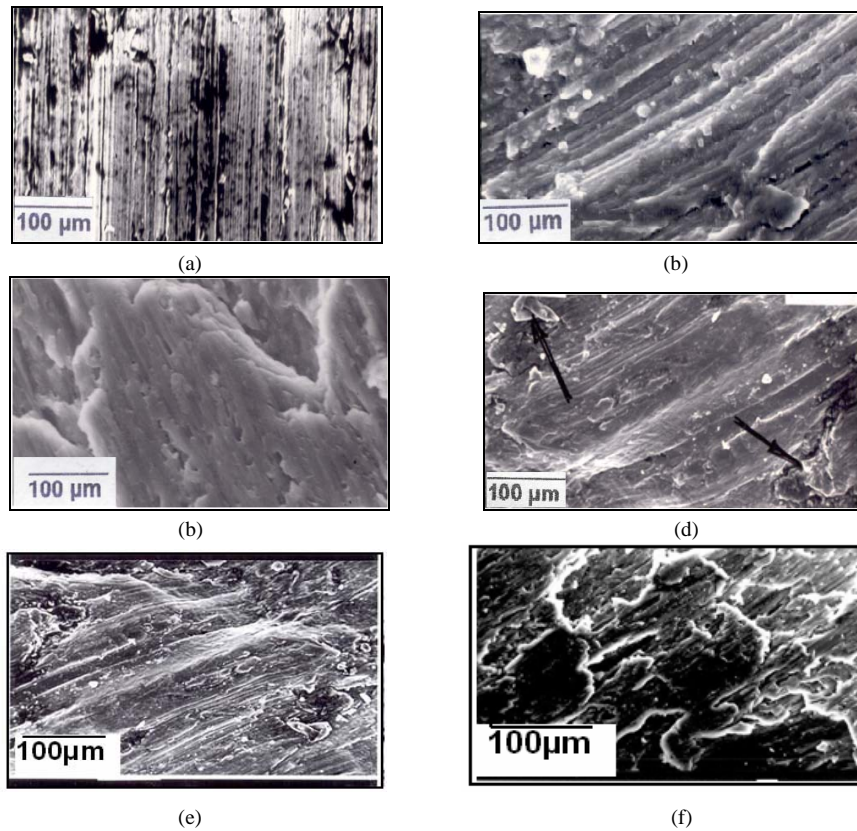
**Figure 5. Wear rate Vs load of matrix alloy and different chilled hybrid MMCs. (a) Plot of wear rate Vs load (Matrix alloy); (b) Plot of wear rate Vs load (Graphite chilled MMCs); (c) Plot of wear rate Vs load (Cu chilled MMCs); (d) Plot of wear rate Vs load (Sub zero chilled MMCs).**

dispersoid tested at loads 10, 30 and 50 N are respectively 0.0025, 0.0074 and 0.009. This checks well with FE predictions as shown in **Figures 7 (a-c)** and **8 (a-c)**.

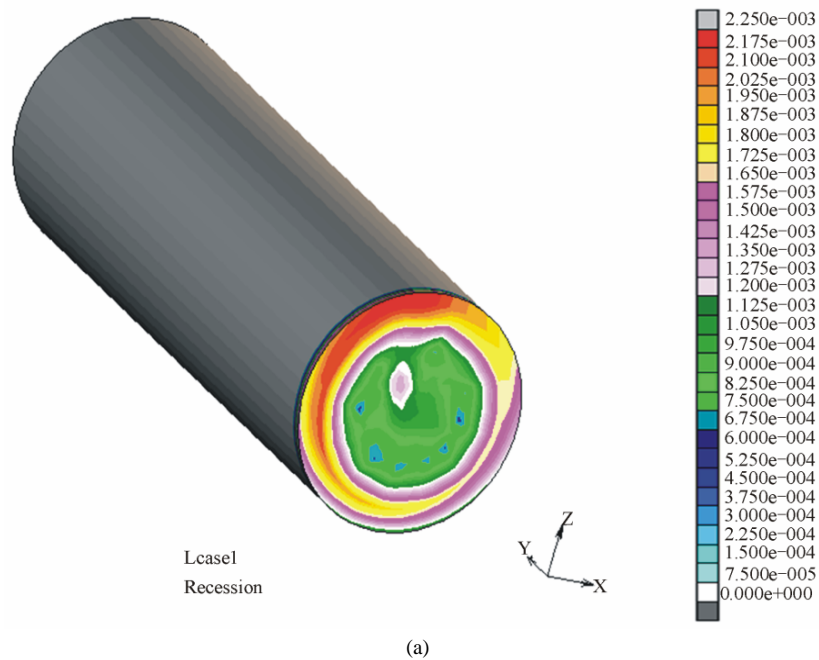
**Figures 6 (a,b)** show typical SEM photographs of the worn surfaces of hybrid composite containing Al<sub>2</sub>SiO<sub>5</sub>-9%/C-3 vol.% and Al<sub>2</sub>SiO<sub>5</sub>-6%/C-3 vol.% dispersoid content cast using sub zero chill tested at a load of 10 N for a time period of 300 seconds. At lower loads (10 and 20 N) the major wear mechanisms of the chilled composite are abrasive and adhesive wear, during which the MMC is worn by the frictional force on the wear surface [42]. At this load it was found that abrasive wear was dominant in ploughing and grooving as indicated in **Figures 6 (a,b)**. It observed that at 10 N load, the MMC with Al<sub>2</sub>SiO<sub>5</sub>-9/C-3 vol.% has grooves formed (**Figure 6(a)**) by the shearing action of the friction on the wear surface. In fact, even the wear surface of the MMC with Al<sub>2</sub>SiO<sub>5</sub>-6/C-3 vol.% dispersoid contains a number of deep wear

grooves (**Figure 6(b)**).

The worn surfaces of the sub zero chilled hybrid MMC containing Al<sub>2</sub>SiO<sub>5</sub>-9/C-3 vol.% and Al<sub>2</sub>SiO<sub>5</sub>-6/C-3 vol.% dispersoid content tested at an intermediate load of 30 N are shown in **Figures 6(c)** and **6(d)**. The wear debris and distorted surface of the MMC with Al<sub>2</sub>SiO<sub>5</sub>-6/C-3 vol.% dispersoid content are more distinct than those in the MMC with Al<sub>2</sub>SiO<sub>5</sub>-9/C-3 vol.% dispersoid content. From the wear surface, it can be seen that the wear debris and distorted surface play an important role on the wear, which increases with their formation and growth. The distorted surface and debris are formed at the locally fractured area of the matrix alloy. This localized fracture is ceased by highly localized frictional forces between the non-uniform surface of the counter material and the defective areas on the wear surface. The wear surface of MMC having Al<sub>2</sub>SiO<sub>5</sub>-6/C-3 vol.% dispersoid content shows severe (see arrow in



**Figure 6.** SEM photographs of sub zero chilled hybrid MMCs tested at different loads. (a) SEM photograph of Al<sub>2</sub>SiO<sub>5</sub>-9/ C-3 vol.% sub zero chilled MMC tested at 10 N; (b) SEM photograph of Al<sub>2</sub>SiO<sub>5</sub>-6/ C-3 vol.% sub zero chilled MMC tested at 10 N; (c) SEM photograph of Al<sub>2</sub>SiO<sub>5</sub>-9/ C-3 vol.% sub zero chilled MMC tested at 30 N; (d) SEM photograph of Al<sub>2</sub>SiO<sub>5</sub>-6/ C-3 vol.% sub zero chilled MMC tested at 30 N; (e) SEM photograph of Al<sub>2</sub>SiO<sub>5</sub>-9/ C-3 vol. % sub zero chilled MMC tested at 50 N; (f) SEM photograph of Al<sub>2</sub>SiO<sub>5</sub>-6/ C-3 vol. % sub zero chilled MMC tested at 50 N.



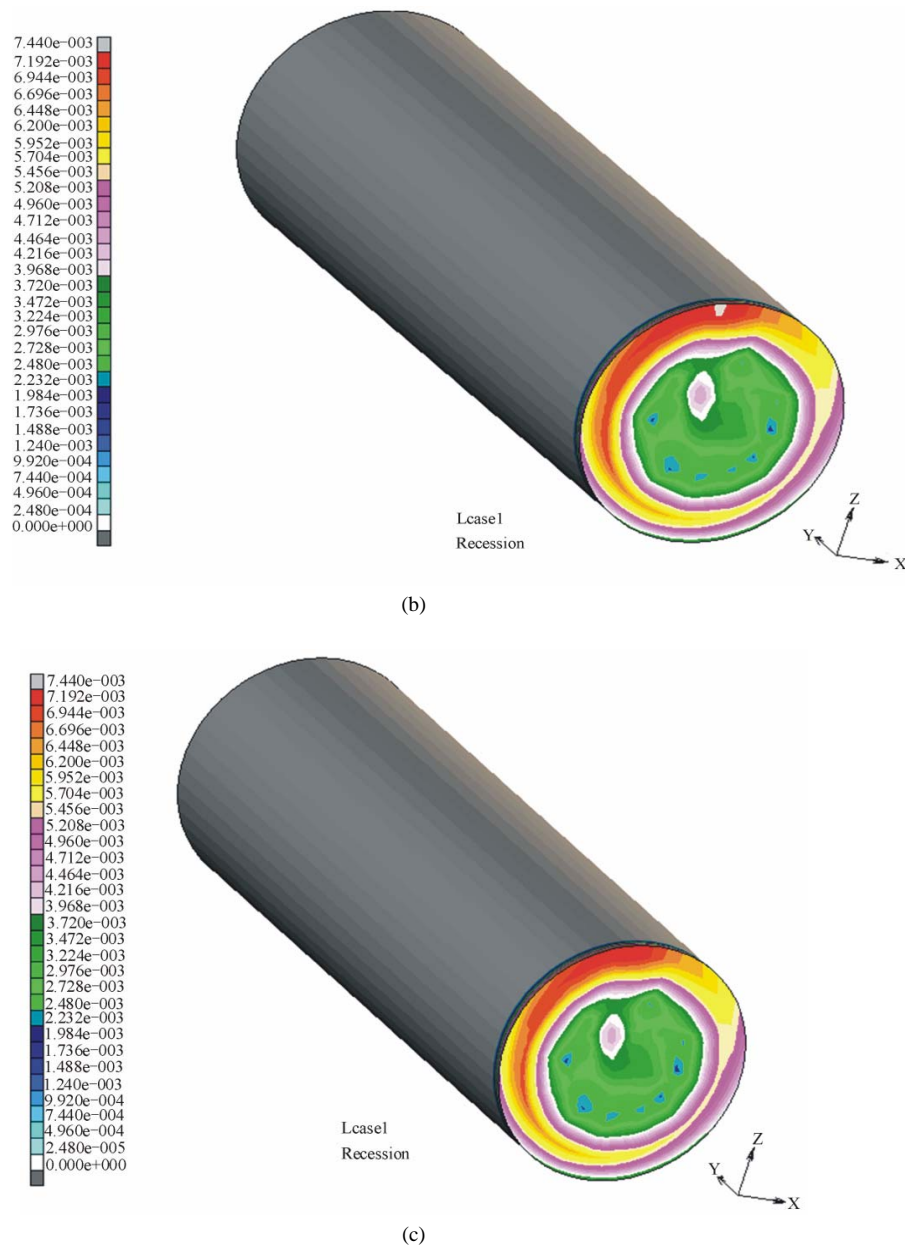


**Figure 7.** (a) Wear Rate (0.00225) of Al<sub>2</sub>SiO<sub>5</sub>-9/C-3 vol.% sub zero chilled MMC for 10 N load; (b) Wear Rate (0.00744) of Al<sub>2</sub>SiO<sub>5</sub>-9/C-3 vol.% sub zero chilled MMC for 30 N load; (c) Wear Rate (0.00929) of Al<sub>2</sub>SiO<sub>5</sub>-9/C-3 vol.% sub zero chilled MMC for 50N load.

**Figure 6(d)** abrasive and adhesive wear which is the dominant wear mechanisms at intermediate load. By contrast, the wear surface of the MMC with Al<sub>2</sub>SiO<sub>5</sub>-9/C-3 vol.% dispersoid content is completely different in that on this surface, abrasive wear is hardly seen (wave like pattern) and this is due to the reduction in frictional forces on the wear surface. Visible lack of damage in both cases (low and intermediate load) is due to the presence of solid lubrication film formed by the addition of carbon particulates on the wear surface of hybrid composites.

Consequently, this result gives rise to the improvement of wear resistance.

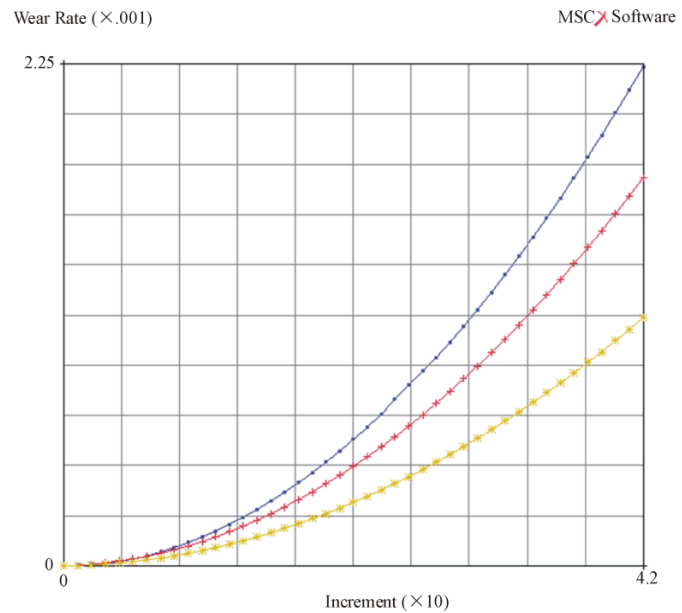
Testing of the chilled MMCs at a final load of 50 N (higher load), however, the major wear mechanism changes to melt wear because of the rise in temperature on the localized wear surface, resulting in the MMCs being worn out less rapidly. At this load the adhesive and slip phenomena also appear (see **Figure 6(e)**). Here, the solid lubricant behavior of carbon makes adhesive wear to be dominant at high sliding speeds. This can be deter-

mined by removed materials and slip phenomena that are found in the wave patterns of materials. The removal of the material seems to be accelerated by fractures of Al<sub>2</sub>SiO<sub>5</sub>/C particulates and the matrix which might be due to the high frictional force on the wear surface. Worn surfaces of Al<sub>2</sub>SiO<sub>5</sub>-9/C-3 vol.% and the Al<sub>2</sub>SiO<sub>5</sub>-6/C-3 vol.% sub zero chilled MMCs tested at a final load of 50 N are shown in **Figures 6(e) and 6(f)** respectively. Localized melted areas (see arrow in **Figure 6(f)**) owing to the rise in temperature can be seen in composite containing Al<sub>2</sub>SiO<sub>5</sub>-6/C-3 vol.% dispersoid. As shown in **Figure 6(f)**, wear of the Al<sub>2</sub>SiO<sub>5</sub>-6/C-3 vol.% dispersoid content

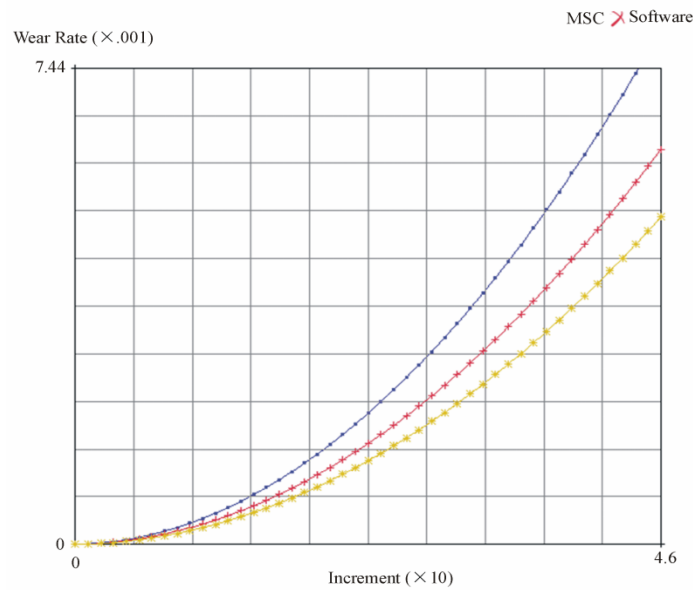
chilled composite seems to start by localized melting of the surface and proceed by delaminations from the matrix in which there is severe plastic deformation. In Al<sub>2</sub>SiO<sub>5</sub>-9/C-3 vol.% chilled composite shown in **Figure 6(e)**, some wave-like wear patterns can be seen which might be related to melt and slip.

#### 4.5. Finite Element Analysis of Wear

MSC Marc software used in the present analysis is equipped with the energy error estimation technique, based on the fact that the FEM structural analysis results in a continuous displacement field from element to



(a)



(b)

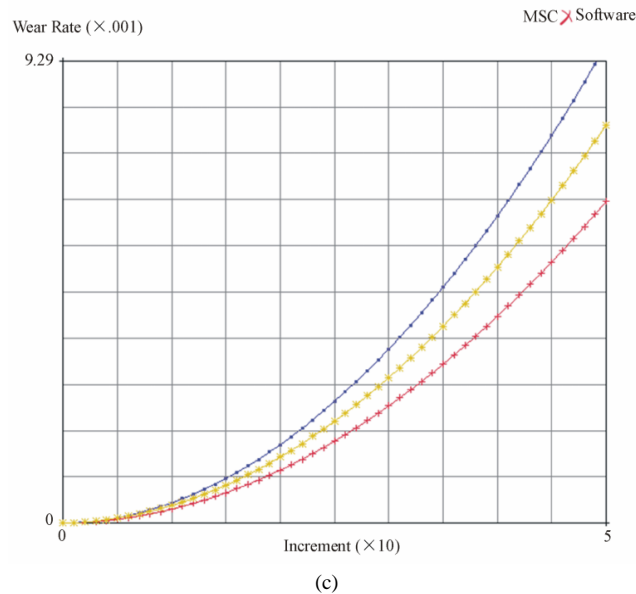


**Figure 8.** Plot of wear rate Vs increment load for Al<sub>2</sub>SiO<sub>5</sub>-9/C-3 vol.% sub zero chilled MMC tested at different loads. (a) Wear Rate Vs Increment load (10 N) × of Al<sub>2</sub>SiO<sub>5</sub>-9/C-3 vol.% sub zero chilled MMC; (b) Wear Rate Vs Increment load (30 N) of Al<sub>2</sub>SiO<sub>5</sub>-9/C-3 vol.% sub zero chilled MMC; (c) Wear Rate Vs Increment load (50 N) of Al<sub>2</sub>SiO<sub>5</sub>-9/C-3 vol.% sub zero chilled MMC.

element, but a discontinuous stress field. To obtain more acceptable stress, the elemental nodal stresses are averaged. The nodal stress error vectors are accordingly evaluated, being a base for the energy error estimation for elements and over the entire model. When the energy errors are equal for every element, then that particular model with its given discretisation is the most effective one.

Perhaps the most convincing way to verify the FEM results is to compare them with the known experimental results. The wear of the pin on disc configuration, **Figure 1**, was analyzed with the FEM approach outlined above. **Figures 7(a-c)** show the evolution of the developed stresses along the sliding direction at different stages of loading as the wear progresses and **Figure 8** shows the wear rate plot. Since we assume that wear is dependent upon stress and the stress values are changing over time due to the wear and the changing contact, then wear at any particular location is changing over time. This can be seen from the contact pressure at different loads representing different amounts of wear as in **Figures 7(a-c)**. In the current configuration, wear is calculated as an update to the state of strain at the end of each sub step. The incremental wear strain would be calculated and would be added to the previously calculated wear strain. Note that changing the loads will require the changing the boundary conditions. The progressive decrease in the contact pressure as the sliding progresses can be qualitatively compared with the ring-on ring case shown in

**Figures 7(a-c)**. However, in the pin-on-disc problem there is a difference in the stress distribution along the sliding direction due to the non-axi-symmetric boundary conditions. This stress distribution is a result of the coefficient and cannot be ignored for the computation of wear. **Figures 8(a-c)** show the graph of wear rate plotted against incremental load perpendicular to the sliding direction. The shape of the particular wear curve for a given contact geometry and loading is determined by the change of the apparent contact area during the rubbing. These figures also show the stress distribution for the initial and final configurations. Finally it can be seen from these graphs that a good agreement exists between the simulated (FE) values and those of the experimental values, proving the suitability of the boundary conditions.

It is seen from **Figures 5(d)**, **7(a-c)** and **8(a-c)** that the experimental wear rate for sub zero chilled MMC containing Al<sub>2</sub>SiO<sub>5</sub>-9/C-3 vol.% dispersoid tested at loads 10, 30 and 50 N checks well with FE predictions.

## 5. Conclusions

In the present research, focusing on mechanical properties and wear of Al/Al<sub>2</sub>SiO<sub>5</sub>/C chilled MMCs, the following points have been highlighted.

Chilled Al/Al<sub>2</sub>SiO<sub>5</sub>/C composites were successfully fabricated by employing various types of chills. It was found that, hardness, strength and wear resistance of the MMC increases as Al<sub>2</sub>SiO<sub>5</sub>/C content increases up to

Al<sub>2</sub>SiO<sub>5</sub>-9 vol.%/C-3 vol.%. Carbon particulates were seen to be less effective in strengthening than when only Al<sub>2</sub>SiO<sub>5</sub> particulates are incorporated.

It is seen from wear analysis that as the load and dispersoid content increases the wear resistance of the composite improves remarkably. SEM studies reveal that wear surfaces of Al/Al<sub>2</sub>SiO<sub>5</sub>/C chilled composite at lower loads showed slight groove formations than those of the matrix alloy. At intermediate loads, damaged sections in wear surfaces of the composites were seldom observed. Consequently, the solid lubrication film formed as a result of adding carbon particulates improved the wear resistance of Al/Al<sub>2</sub>SiO<sub>5</sub>/C hybrid composites. At higher loads, localized melt and slip and large plastic deformations are the dominant factors contributing the removal of the material. Comparison with experiments has confirmed the stability of the FE wear model developed, the model provides a reasonable description and justification.

## REFERENCES

- [1] H. C. Yuen and W. B. Lee, "Hot bonding Al Matrix Composite with Different Fraction of Alumina," *Material Science*, Vol. 30, 1995, pp. 843-849. [doi:10.1007/BF01178415](https://doi.org/10.1007/BF01178415)
- [2] H. C. Yuen, B. Ralph and W. B. Lee, "Novel Preparation for an Aluminum-Alumina MMC by a Hot Roll Bonding Process," *Scripta Metallurgica et Materialia*, Vol. 29, 1993, pp. 695-670. [doi:10.1016/0956-716X\(93\)90421-N](https://doi.org/10.1016/0956-716X(93)90421-N)
- [3] B. Ralph, H. C. Yuen and W. B. Lee, "The Processing of MMCs: An Overview," *Materials Processing Technology*, Vol. 63, 1997, pp. 1-8. [doi:10.1016/S0924-0136\(96\)02645-3](https://doi.org/10.1016/S0924-0136(96)02645-3)
- [4] Z. G. Wei, C. Y. Tang and W. B. Lee, "Design and Fabrication of Intelligent Composites Based on Shape," *Materials Processing Technology*, Vol. 63, 1997, pp. 68-75. [doi:10.1016/S0924-0136\(96\)00041-6](https://doi.org/10.1016/S0924-0136(96)00041-6)
- [5] Y. P. Rao and W. B. Lee, "Processing a Particulate MMC by Roll Bonding Method, Discussion Meeting on Inorganic Matrix Composites," Indian Institute of Science, Bangalore, India, No. 3, 1995, pp. 8-18.
- [6] K. Yeow, "Transaction Behavior of Unidirectional Ribbon Reinforced Metal Glass Epoxy Laminates," *Composite Materials*, Vol. 14, 1980, pp. 132-139. [doi:10.1177/002199838001400110](https://doi.org/10.1177/002199838001400110)
- [7] B. D. Agarwal and J. M. Lifshitz, "Elastic-Plastic Finite Element Analysis of Short Fiber Composites," *Fiber Science and Technology*, Vol. 7, 1974, pp. 45-53. [doi:10.1016/0015-0568\(74\)90005-0](https://doi.org/10.1016/0015-0568(74)90005-0)
- [8] T. G. Neigh and D. J. Chellman, "Modulus Measurements in Discontinuous Reinforced Al Composites," *Scripta Metallurgica*, Vol. 18, 1984, pp. 925-931. [doi:10.1016/0036-9748\(84\)90262-X](https://doi.org/10.1016/0036-9748(84)90262-X)
- [9] A. P. Divecha, S. G. Fishman and S. D. Karmarkar, "Silicon Carbide Reinforced Al: A Formable Composite," *Journal of Metals*, Vol. 12, 1981, pp. 12-17.
- [10] D. L. McDaniels, "Analysis of Stress-Strain, Fracture and Ductility Behavior of Al MMCs Containing Discontinuous Silicon Carbide Reinforcement," *Metallurgical Transactions A*, Vol. 16A, 1985, pp. 1105-1113. [doi:10.1007/BF02811679](https://doi.org/10.1007/BF02811679)
- [11] D. R. Williams and M. E. Fine, "Quantitative Determination of Fatigue Microcrack Growth in SiC Whisker Reinforced 2124 Al Alloy Composites," *Proceedings of ICCM-V*, San Diego, CA, AIME, TMS, Vol. 29, 1958, pp. 639-645.
- [12] J. Hemanth, "Cryo Effect during Solidification on the Tribological Behavior of Al-Alloy/Glass (SiO<sub>2</sub>) MMCs," *Journal of Composite Materials*, Sage publications, Vol. 43, 2009, pp. 675-688.
- [13] J. Hemanth, "Tribological Behavior of Cryogenically Treated Al-12%Si Alloy/B4C Composites," *Wear*, Elsevier Science, Vol. 258, 2005, pp. 1732-1745. [doi:10.1016/j.wear.2004.12.009](https://doi.org/10.1016/j.wear.2004.12.009)
- [14] J. Hemanth, "Cryogenic Effects during Solidification on the Wear Behavior of Al Alloy/Glass MMCs," *Journal of Composite Materials Part A*, Vol. 38, 2007, pp. 1395-1402.
- [15] J. Hemanth, "Development and Property Evaluation of Al-Alloy Reinforced with Nano-ZrO<sub>2</sub> Metal Matrix Composites (NMMCs)," *Journal of Materials Science and Engineering A*, Vol. 507, 2009, pp. 110-113. [doi:10.1016/j.msea.2008.11.039](https://doi.org/10.1016/j.msea.2008.11.039)
- [16] R. G. Schierding and O. D. Deex, "Factors Influencing the Properties of Whisker-Metal Composites," *Composite Materials*, Vol. 3, 1969, pp. 618-625.
- [17] T. T. Long, T. Nishimura and T. Aisaka, "Mechanical Properties and Wear Resistance of 6061 Al Alloy Reinforced with Hybrid Fibers and Whiskers," *Transactions of Japan Institute of Metals*, Vol. 29, 1988, pp. 920-928.
- [18] R. J. Arsenault, "The Strengthening of Al Alloy 6061 by Fiber and Platelet SiC," *Materials Science and Engineering*, Vol. 64, 1984, pp. 171-178. [doi:10.1016/0025-5416\(84\)90101-0](https://doi.org/10.1016/0025-5416(84)90101-0)
- [19] S. V. Nair, J. K. Tien and R. C. Bates, "SiC Reinforced Al MMCs" *Institute of Metals*, Vol. 30, 1985, pp. 275-283.
- [20] J. Hemanth, "Quartz (SiO<sub>2</sub>p) Reinforced Chilled Metal Matrix Composites (CMMCs) for Automotive Applications," *Materials and Design*, Elsevier Science, Vol. 30, 2009, pp. 323-329.
- [21] J. Hemanth, "Development and Property Evaluation of Al-Alloy Reinforced with Nano-ZrO<sub>2</sub> Metal Matrix Composites for Automotive Applications," *SAE International world congress*, Paper No. 2009-01-0218, Detroit, Michigan, USA, 2009.
- [22] A. Razaghian, D. Yu and T. Chandra, "Fracture Behavior of a SiC Particle Reinforced Al Alloy at High Temperature," *Composites Science and Technology*, Vol. 58, 1998, pp. 293-298. [doi:10.1016/S0266-3538\(97\)00130-9](https://doi.org/10.1016/S0266-3538(97)00130-9)
- [23] S. Q. Wu, H. Z. Wang and S. C. Tjong, "Wear Behavior Al Based Composites Reinforced with Ceramic Particles," *Composites Science and Technology*, Vol. 56, 1996,

- pp. 1261-1268. [doi:10.1016/S0266-3538\(96\)00085-1](https://doi.org/10.1016/S0266-3538(96)00085-1)
- [24] S. C. Tjong, S. Q. Wu and H. C. Liao, "Wear Behavior of Al-12%Si Alloy Reinforced with a Low Volume of SiC Particles," *Composites Science and Technology*, Vol. 57, 1997, pp. 1151-1158
- [25] C. M. Friend, "The Effect of Alumina Fiber Array on the Age Hardening Characteristics of and Al/Mg/Si Alloy," *Materials Science*, Vol. 22, 1987, pp. 3005-3012. [doi:10.1007/BF01086505](https://doi.org/10.1007/BF01086505)
- [26] J. M. Thompson, "A Proposal for the Wear Calculation," Department of Mechanical engineering, MIT, 2007, pp. 45-57.
- [27] P. Podra and S. Anderson, "Simulating Sliding Wear with Finite Element Method," *Tribology International*, Vol. 32, 1999, pp. 71-81. [doi:10.1016/S0301-679X\(99\)00012-2](https://doi.org/10.1016/S0301-679X(99)00012-2)
- [28] G. E. Lee, C. K. H. Dharan and R. O. Ritchie, "A physically Based Abrasive Wear Model for Composite Materials," *Wear*, Vol. 252, 2002, pp. 322-331. [doi:10.1016/S0043-1648\(01\)00896-1](https://doi.org/10.1016/S0043-1648(01)00896-1)
- [29] K. Elleuch and S. Fouvry, "Experimental and Modeling Aspects of Abrasive Wear of a A357 Aluminum Alloy under Gross Slip Fretting Conditions," *Wear*, Vol. 258, 2005, pp. 40-49. [doi:10.1016/j.wear.2004.04.010](https://doi.org/10.1016/j.wear.2004.04.010)
- [30] J. Hemanth, "Wear Characteristics of Sub Zero Chilled Cast Iron," *Wear*, Vol. 192, 1996, pp. 134-143. [doi:10.1016/0043-1648\(95\)06781-7](https://doi.org/10.1016/0043-1648(95)06781-7)
- [31] J. Hemanth, "Effect of Cooling Rate on the Dendrite Arm Spacing and Ultimate Tensile Strength of Cast Iron," *Material Science*, Vol. 33, 1998, pp. 23-35. [doi:10.1023/A:1004321007806](https://doi.org/10.1023/A:1004321007806)
- [32] J. Hemanth, "Effect of High Rate of Heat Transfer during Solidification of Alloyed Cast Iron Using Water-Cooled and Sub-Zero Chills on Mechanical Behavior," *Materials and Design* Vol. 24, 2003, pp. 37-45. [doi:10.1016/S0261-3069\(02\)00086-9](https://doi.org/10.1016/S0261-3069(02)00086-9)
- [33] J. F. Archard and W. Hirst, "The Wear of Metals under Un-Lubricated Conditions," *Proceedings of the Royal Society-A, Mathematical, Physical and Engineering Sciences*, Vol. 236, 1956, pp. 397-410. [doi:10.1098/rspa.1956.0144](https://doi.org/10.1098/rspa.1956.0144)
- [34] J. J. Lewandowski, C. Liu and W. H. Hunt, "Microstructure Effects on the Fracture Micro-Mechanisms in Al MMCs in Processing and Preparation for Powder Metallurgy Composites," P. Kumar and A. Ritter, Eds., *TMS*, Vol. 12, 1988, pp. 117-128.
- [35] M. Taya and R. J. Arsenault, "Heat Treating of Composite Materials," *Composite materials*, Pergamon press, Vol. 35, 1989, pp. 56-67.
- [36] B. Ralph, H. C. Yuen and W. B. Lee, "Mechanical Properties and Microstructure of Composite Materials," *Materials Processing Technology*, Vol.63, 1997, pp. 9-18.
- [37] V. G. Gorbounov and V. D. Parshin, "Sliding Wear Characteristics of Al/SiO<sub>2</sub> Composites," *Russian Casting Production*, Vol. 35, 1974, pp. 348-356
- [38] T. G. Neigh, "Wear Regimes and Transition in Al<sub>2</sub>O<sub>3</sub> MMCs," *Metallurgical and Materials Transactions*, Vol. 15, 1984, pp. 139-146.
- [39] P. K. Ghosh and S. K. Ray, "Wear Behavior of Al-12%Si Alloy Reinforced with Low Volume Fraction of SiO<sub>2</sub> Particles," *Materials Science*, Vol. 21, 1986, pp. 1167-1175.
- [40] E. Rabinowicz, "Friction Wear of Materials," John Wiley and Sons, New York, Vol. 32, 1965, pp. 168-177.
- [41] J. F. Archard, "Properties of Composite Materials" *Journal of Applied Physics*, Vol. 24, 1953, pp. 981-988. [doi:10.1063/1.1721448](https://doi.org/10.1063/1.1721448)
- [42] A. G. Wang and I. M. Hutchings, "Wear of Alumina-Fiber Aluminum Composites," *Materials Science and Technology*, Vol. 5, 1989, pp. 71-84.